

## NUMERICAL HEAT FLUX ANALYSIS OF A TROMBE WALL SYSTEM IN TURKEY

Ercan Şerif KAYA \*

Received: 19.08.2021; revised: 14.02.2022; accepted: 23.04.2022

**Abstract:** Trombe wall is an inexpensive passive heating design method used for storing and utilizing solar energy to increase indoor temperature without relying on any mechanical system that requires additional energy. Most recent studies concerning solar wall configuration and energy efficiency have been conducted by using computational fluid dynamics. One reason for this is because semi-transparent and opaque boundaries are provided in simulating wall and glazing surfaces around the fluid domain and solar heat flux energy are allowed in through semi-transparent boundaries. However, finite element method programs employ solid and shell elements as opaque walls that transmit the energy into the domain. In this study, numerical heat flux analysis of a Trombe wall system, which was built for a previous experimental study, has been performed and numerical and experimental analysis results have been verified. According to the simulation studies, heat transfer analysis results are obtained in a good agreement with real time measurements when additional solar load calculated due to transmissivity are defined at the surfaces which are expected to be sun exposed. Besides, numerically verified model of the Trombe wall system was used in evaluating energy saving potential of residential buildings for three cities with different climate regions in Turkey.

**Keywords:** Passive heating system, Trombe wall, Heat flux, CFD, FEM, Solar energy

### Türkiye'deki Tromb Duvar Sistemine ait Sayısal Isı Akısı Analizi

**Öz:** Tromb duvar, güneş enerjisinin depolanarak iç ortam sıcaklığının ilave enerji tüketimi gerektiren herhangi bir mekanik sisteme bağımlı kalmaksızın artırılması için kullanılan pahalı olmayan bir pasif ısıtma sistemidir. Son zamanlarda ısı duvarının konfigürasyon ve enerji verimliliğine yönelik yapılan çalışmaların çoğu hesaplamalı akışkanlar dinamiği yardımıyla gerçekleştirilmiştir. Bunun sebeplerinden bir tanesi, bu programlarda cam ve akışkan alan çevresindeki yüzey sınır koşullarının temsil edildiği yarı geçirgen ve geçirimsiz duvarların kullanıcıya sağlanması ve enerjinin sadece yarı geçirgen duvarlar içerisinden geçebilmesine izin verilmesidir. Ancak, sonlu elemanlar metodu programlarında geçirimsiz duvar özelliklerine karşılık gelen ve enerjiiyi ısı akısı şeklinde aktaran katı ve kabuk elemanlar kullanılabilir. Bu çalışmada, daha önce deneysel bir çalışma kapsamında inşa edilmiş Tromb duvarı sistemine ait sayısal ısı akısı analizi gerçekleştirilmiş ve sayısal analiz deneysel analiz sonuçları ile doğrulanmıştır. Simülasyon çalışmalarına göre, güneş ışığı alması beklenen yüzeylere geçirgenlik katsayısına bağlı olarak hesaplanacak ilave güneş enerjisi tanımlanması halinde elde edilen sonuçların deneysel çalışmalarla örtüştüğü görülmüştür. Bununla birlikte, sayısal olarak doğrulanmış Tromb duvar modelinin kullanılarak Türkiye'deki üç farklı iklim bölgesine ait konut yapılarındaki enerji tasarruf potansiyelinin değerlendirilmesine yönelik bir çalışma yapılmıştır.

**Anahtar Kelimeler:** Pasif ısıtma sistemleri, Tromb duvar, Isı akısı, CFD, FEM, Güneş enerjisi

## 1. INTRODUCTION

The building industry originated energy consumption gives rise not only to environmental issues on the global scale but also to increasing energy demand and costs. Therefore, sustainable and energy efficient passive solar systems have become more important to reduce carbon emissions and energy costs. Trombe walls (TWs) are one of the most widely adopted passive solar systems that utilize solar energy both in heating and cooling (Gupta and Tiwari, 2016). TWs mainly consist of four major components which are glazing, air space/channel, thermal mass and vents. The working principle of the TW is illustrated in Figure 1. The Trombe wall is south facing for maximum solar energy absorption through dark-colored surface, and interior space temperature is increased by the heat transfer process. Besides, as the air in the air space gets warmer, a full circulation begins through the vents into the room due to density changes.

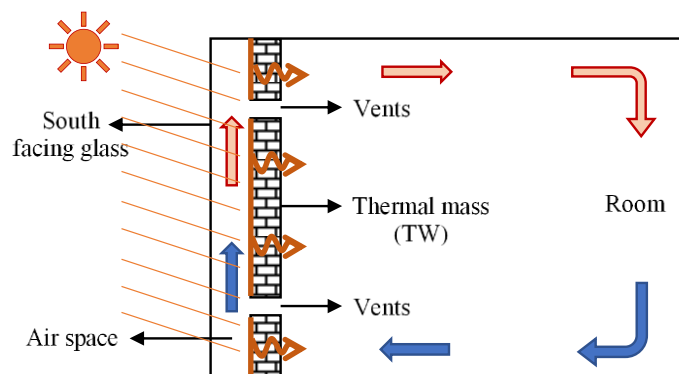


**Figure 1:**  
*Major components and air circulation mechanism of the Trombe wall*

In the literature, a lot of studies were conducted to analyze these components and their effects on thermal performance of solar wall systems. Some of these studies have employed conventional numerical analysis and experimental methods (Yilmaz and Kundakci, 2018; Stazi et al., 2012; Gan, 1998; Ozbalta and Kartal, 2010; Fang and Li, 2000; Briga et al., 2008; Demirbilek et al., 2003) in optimizing system configuration through above mentioned components.

Glazing unit variations including single glazed (Yilmaz and Kundakci, 2018) and double glazed (Stazi et al., 2012) windows installed with Argon and Low-E coating were implemented in solar wall systems. It is noted that an appropriate glazing design can significantly reduce energy cost throughout all year under various climates. Air channel which corresponds to the small space between glazing and thermal wall was also investigated (Yilmaz and Kundakci, 2018; Gan, 1998) based on different interspace values. According to the results, it is suggested that the effective length of the air space to be taken around 10 to 15 cm and increasing the interspace distance has only limited effect in thermal conditions. As for thermal mass, material effect (Stazi et al., 2012) accompanied with surface colors (Ozbalta and Kartal, 2010) and thickness effect (Fang and Li, 2000; Briga et al., 2008) has been taken into consideration in order to increase heat storage capacity. There is also a relatively complex structure compared to traditional buildings, subjected to thermal optimization studies (Demirbilek et al., 2003) by taking into consideration of glazing, thermal wall thickness, window/wall ratio and insulation material selections all at once. Phase change materials have also been used lately in improving Trombe wall efficiency by several researchers (Xiong et al., 2022; Duan et al., 2021)

On the other side, CFD programs are often used by researchers when dealing with temperature distribution, air flow/circulation and ventilation problems where density changes and buoyancy effect get involved (Jaber and Ajib, 2011; Kaya et al., 2021). In this manner, vent

optimization related research studies have employed and taken advantage of CFD fluent environments. A research study with regard to vent management (Jaber and Ajib, 2011) investigating optimum opening and closing times for air vents was conducted to prevent energy losses and optimize stored heat energy for the periods before and after sunset/sunrise. In spite of a large number of research studies undertaken, yet only few referred how to adjust vent size and dimensions for obtaining optimum performance (Briga et al., 2014; Jaber and Ajib, 2011). A recent study (Kaya et al., 2021) has pointed out this research gap and investigated the effect of total vent/wall area ratio on TWs thermal performance by increasing this ratio by 2% starting from unvented case. The results showed that any TW configuration with 8% vent/wall ratio provides maximum heating performance.

In parallel with the ease of simulating fluid flow problems, CFD programs provide solar ray tracing algorithms and solar load modules (ANSYS, 2013) that allow the users to apply solar transmission determined over the course of a day for any given geographical location with a specified date (Liu et al., 2013, Hernandez et al., 2016; Bajc et al., 2015; Blotny and Nems, 2019; Simones et al., 2021). Besides, semi-transparent and opaque boundary conditions can be adopted to simulate wall and glazing properties by taking transmissivity, reflectivity and absorptivity into consideration. Moreover, solar load module provides the users both fair and theoretical maximum weather conditions to represent expected atmospheric conditions during simulations (ANSYS, 2013)

ABAQUS software as finite element method tool is also employed in simulating heat transfer process where the heat exchange between envelopes and surrounding air mainly governed by heat convection, heat radiation and heat conduction through the building envelope. For example, thermal performance analysis of a three-story building (Zhou et al., 2014) with thermal insulating concrete wall panel has examined and indoor temperature assumed to be similar to the interior wall surface temperature so that energy savings can be predicted due to maximum interior surface temperature. Another experimental heat flux analysis study was performed to quantify the radiation and convection exchanges for different elements (Dimassi and Dehmani, 2016). There are also some research studies comparing ANSYS and ABAQUS software in modeling contact issues (Yaylaci ve Avcar, 2020; Yaylaci vd., 2020).

The main difference when modeling solar walls by using CFD and FEM programs is that solar load model in Fluent allows the solar heat flux transmission through all glazed surfaces by means of semi-transparent walls whereas no transmittance is allowed in finite element models. In this study, a numerical heat flux analysis of a Trombe wall is conducted in simulating and verifying a previous experimental test room by using finite element method. It is seen that the results can be obtained in accordance with real measurements when additional heat flux load is defined in surfaces which are expected to be sun exposed. For this purpose, solar radiation calculations were carried out to be applied on glazing surface and additional solar heat flux load is calculated taking into consideration of transmissivity. Besides, verified three-dimensional (3D) finite element model of the Trombe wall system is used in evaluating energy saving potential of residential buildings for three cities with different climate regions in Turkey. And for simplicity, it is assumed that the interior surface temperature of the TW is equal to the indoor temperature.

## **2. EXPERIMENTAL SETUP AND MEASUREMENT**

An actual test room built for a previous experimental study was chosen as a case study and modeled by using finite element method program to be used in verification studies. Figure 2 illustrates the experimental test room (Fig. 2.a) which is a Solar house located in Istanbul, integrated TW system (Fig. 2.b), and the 3D finite element model of the test room which is 3.0 m both in length and width, and 3.3 m in height. The solar wall is 15 cm in thickness and there are 8 vents positioned in two line one in the upper and the other in the lower part of the wall. All

vents are 50 cm x 20 cm in dimensions and aligned with a 15cm distance from both top and bottom edges and temperature measurement points are located one meter away from the near wall edges by using K-type thermocouples (Fig. 2.c). The spaces between vents are also set to be 25 cm. Besides, the distance between TW and glazing is 20 cm (Fig. 2.d). All components of the experimental setup including roof, floor and exterior walls are made out of concrete (Ogus, 2013).

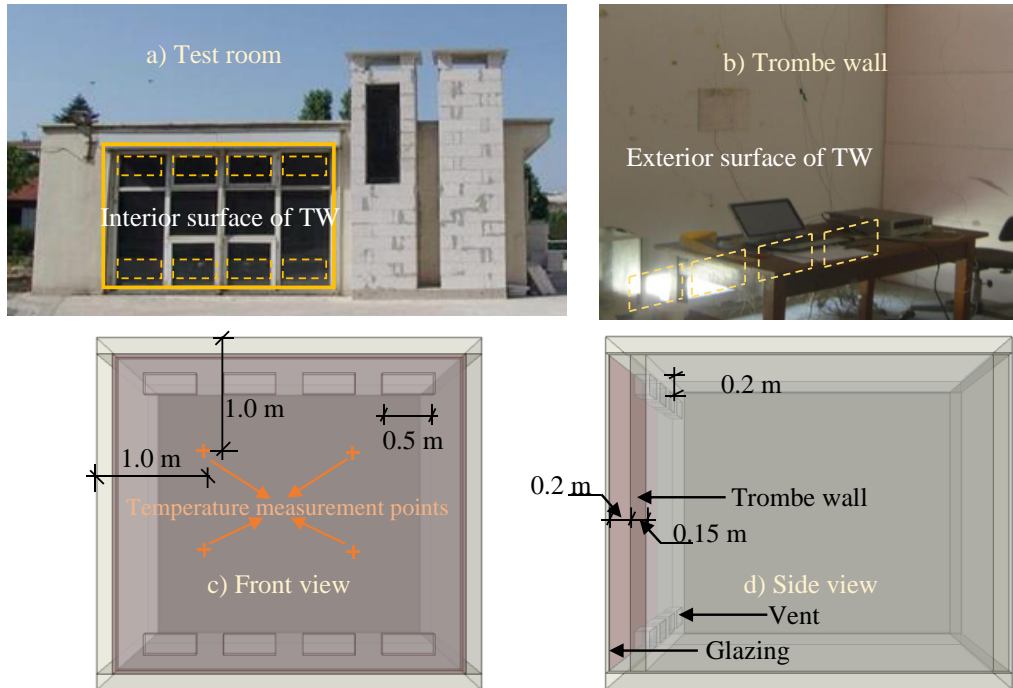


**Figure 2:**

*A view of a) experimental test room and b) exterior surface of the TW (Ogus, 2013), c) front view of the finite element model and d) dimensions of major components*

The Trombe wall integrated part of the Solar house (with an 170° of azimuth angle) was monitored to obtain glazing, interior and exterior surface temperatures of the thermal wall for the period between 5<sup>th</sup> of April and 12<sup>th</sup> of April 2013 (Ogus, 2013). As can be seen in Figure 3, the 8<sup>th</sup> and 9<sup>th</sup> of April represent cloudy days with minimum temperature records while the maximum surface temperatures were obtained on 6<sup>th</sup> of April as 44.4 °C, 44.1 °C and 27.6 °C for glazing, exterior and interior surfaces of the TW, respectively. These maximum surface temperatures were selected as evaluation criteria and an extensive trial and error process were practiced through numerical heat flux analysis to develop a rigorous finite element model which is capable of simulating solar wall problems accurately as in CFD environments and experimental studies.

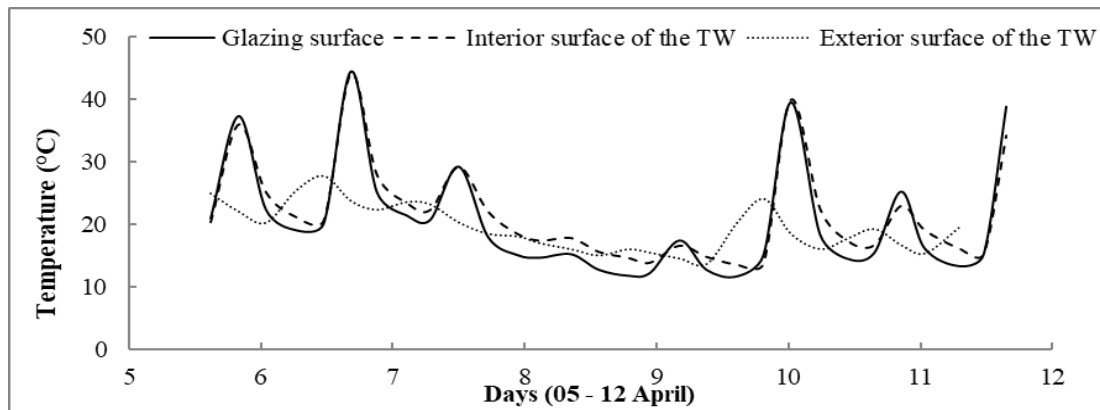


**Figure 3:**  
Temperature measurements on the glazing, interior and exterior surfaces of the TW

### 3. THE 3-D FINITE ELEMENT ANALYSIS

The three-dimensional finite element model, which is created identical with the experimental model, was simulated by using ABAQUS software to investigate the thermal behavior. Heat exchange between surrounding air and envelopes of the test room is taken place mainly by means of radiative and convective heat transfer, and by conductive heat transfer along the building envelope. Therefore, average hourly ambient temperature and solar radiation calculations for the month of April were estimated and used as input data.

In reality, ambient temperature varies every single day and hours. However, this data for the corresponding experiment dates was not provided. Therefore, the average daily temperature values of the test site were taken via Photovoltaic Geographical Information System (PGIS, 2021) at latitude/longitude: 41.015°N/28.979° E, on hourly basis and employed as ambient temperature for the numerical heat transfer analysis in between 8:00 am to 17:00 pm (Fig. 4).

Solar radiation is another important and basic parameter that should be estimated and defined on glazing surface as heat flux load. There are several models proposed to estimate incident solar radiation on inclined surfaces since most of the surfaces where solar energy is converted to heat or electricity in solar energy applications are placed inclined. In this study, Liu and Jordan's estimation model (Liu and Jordan, 1961) has been adopted in calculating solar radiation loads. According to this model, the total hourly solar radiation ( $I_{TE}$ ) on inclined surface is the sum of beam ( $I_{BE}$ ), diffuse ( $I_{DE}$ ) and reflected ( $I_{RE}$ ) radiation as given below (1),

$$I_{TE} = I_{BE} + I_{DE} + I_{RE} \quad (1)$$

However, Trombe wall glazing is placed in a vertical direction. Therefore, the slope of the surface is taken as ( $\beta = 90^\circ$ ) in calculations. Besides, incident solar ratio on inclined surface is obtained by multiplying beam radiation on horizontal surface ( $I_B$ ) and the ratio of beam radiation ( $R_B$ ).

$$I_{BE} = I_B R_B \quad (2)$$

The ratio of beam radiation ( $R_B$ ) on inclined surfaces can be defined as following equation.

$$R_B = \text{Cos}(\theta) / \text{Cos}(\theta_z) \quad (3)$$

The angle of incidence ( $\theta$ ) and the solar zenith angle ( $\theta_z$ ) is calculated by following Eq. (4) and Eq. (5) where ( $d$ ) is declination, ( $\phi$ ) is latitude, ( $\beta$ ) is slope and ( $w$ ) is hour angle.

$$\text{Cos}(\theta_z) = \sin(d) \sin(e) + \cos(d) \cos(e) \cos(w) \quad (4)$$

$$\text{Cos}(\theta) = \sin(d) \sin(e - \beta) + \cos(d) \cos(e - \beta) \cos(w) \quad (5)$$

Eq. (6) is also given for calculating the declination angle due to ( $n$ ) parameter which is equal to the nth day of the year starting from January the first.

$$d = 23.45 \text{ Sin } (2\pi n (n + 284) / 365) \quad (6)$$

Diffused and reflected solar radiation can also be calculated due to Eq. (7) and Eq. (8).

$$I_{DE} = \frac{1}{2} \cdot I_D (1 + \text{Cos}\beta) \quad (7)$$

$$I_{RE} = \frac{1}{2} \cdot I_D (1 - \text{Cos}\beta) \quad (8)$$

Estimated solar radiation vs. average ambient temperature values are plotted in Fig. 4 and were used in the steady state heat transfer analysis. The outcomes of the numerical heat flux analysis were validated with actual temperature measurements of the test room.

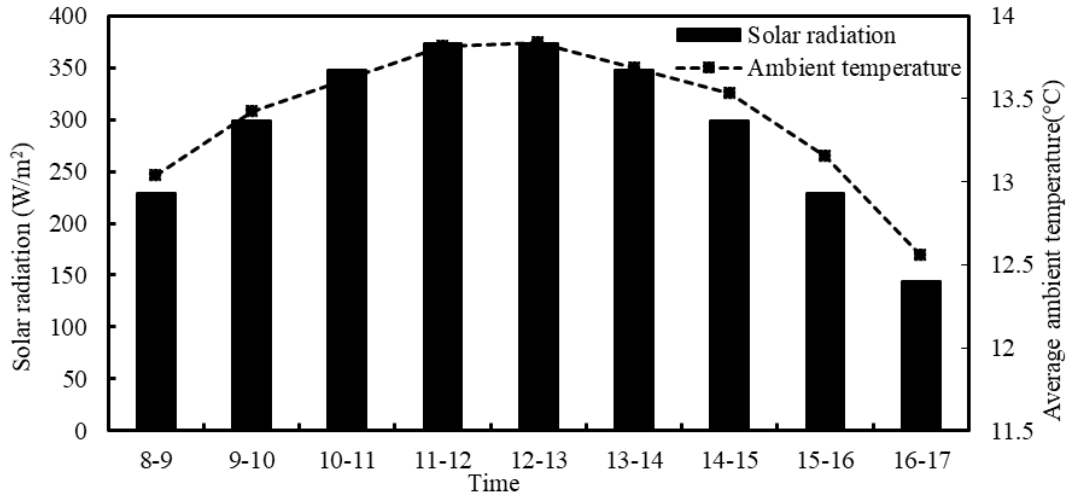


**Figure 4:**  
*Estimated solar radiation and ambient temperatures for the month of April*

The main components of the three-dimensional finite element model including floor, roof, exterior walls, thermal wall and glazing are merged in one structure. And all structure surfaces are set to be in contact with ambient air. Each material properties employed in creating simulation model of the test setup are summarized in Table 1.

**Table 1. Material properties used for numerical studies**

Material	Density (kg/m <sup>3</sup> )	Specific Heat (J/kg.K)	Thermal Conductivity (W/m.K)
Air	1.225	1006.43	0.024
Concrete	2000.0	960.00	1.20
Glass	2500.0	840.00	0.81

Concrete material is modeled with a thermal conductivity, ( $k$ ) of 1.20 (W/mK) whereas, thermal conductivity properties of glazing and air materials are set to be 0.81 and 0.024 (W/mK). Specific heat ( $c_p$ ) values are taken 960.00, 840.00 and 1006.43 (J/kgK) for concrete, glass and air materials, respectively (Table 1.). Film conditions to represent heat loss from surfaces due to air convection are defined as 20.00 and 7.00 (W/m<sup>2</sup>K) at the outside and inside surfaces, respectively as suggested in the German Standard specified for heating requirements for buildings (DIN, 1980), Table 2.

**Table 2. Technical properties of boundary conditions used in numerical studies**

Boundary Name	Heat-Transfer coefficient (W/m <sup>2</sup> /K)	Thermal Conductivity (W/m)/K	Absorption coefficient (m <sup>-1</sup> )	Transmissivity (-)
Glazing (Glass)	7.0	0.81	0.00	0.81
Walls (Concrete)	20.0	1.20	1.70	-
Roof (Concrete)	20.0	1.20	200.00	-
Floor (Concrete)	-	1.20	-	-

Additional material parameters which are used for the 3D model are as given as follows: emissivity of concrete, ( $\epsilon_c$ ) is 0.94 and Stefan-Boltzmann constant,  $\sigma$  is  $5.67 \times 10^{-8}$  (Wm<sup>-2</sup>K<sup>-4</sup>).

DC3D8, an 8-node linear heat transfer brick element is employed with hexagonal element shape in the room for the model discretization. The proposed approach in simulating solar load module in solid/shell elements is to apply solar radiation load calculated by estimation models on glazing surface and defining additional solar heat flux representing transmitted radiation on the Trombe wall surface which is/are expected to be sun exposed. In this purpose, estimated solar radiation values are multiplied by glazing transmissivity factor which assumed to be ( $\tau_g$ ) 0.81 for this research study and applied on numerical model as seen in Fig. 5. Besides, thermal interaction is defined to allow thermal exchange between each instance and environment. Ambient temperature and solar radiation both on glazing surface and Trombe wall surface representing transmitted radiation through glazing were defined as initial conditions.

**Table 3. Parameters used in numerical studies**

	Istanbul (41.015°N/28.979°E)	Ankara (39.898°N/32.778°E)	Antalya (36.895°N/30.655°E)
Temperature (C°)	T <sub>OUT</sub> 7.63	T <sub>OUT</sub> 6.52	T <sub>OUT</sub> 10.80

Heat Flux Load (W/m <sup>2</sup> )	Glazing surface	Interior surface of TW	Glazing surface	Interior surface of TW	Glazing surface	Interior surface of TW
		366.80	$366.80 * 0.81 = 297.11$	368.90	$368.90 * 0.81 = 298.09$	374.30
Heating Degree Days (HDD)	February	Yearly	February	Yearly	February	Yearly
	300	1550	400	2182	182	734

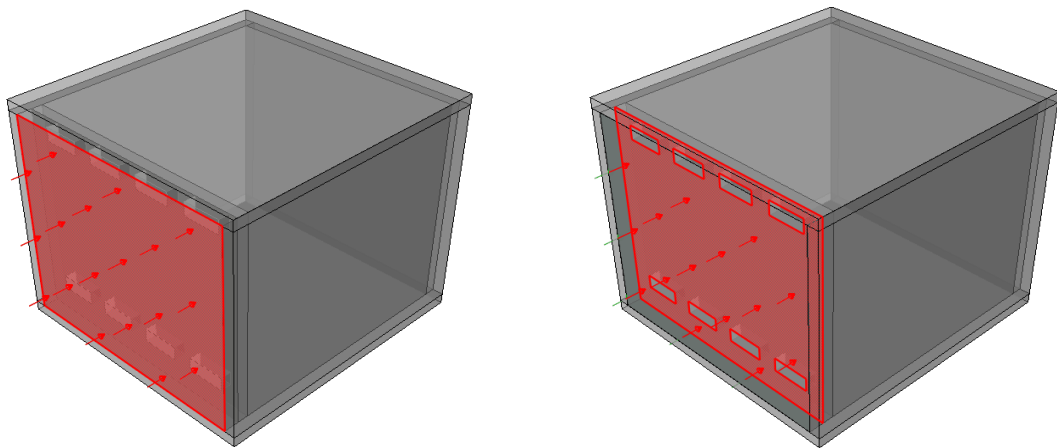


**Figure 5:**  
Solar radiation definition on glazing surface (left) and additional solar heat flux on the sun exposed surface of TW (right)

#### 4. NUMERICAL ANALYSIS RESULTS AND VALIDATION STUDIES

Maximum outside temperature at between 12:00 and 13:00 o'clock is taken 13.84 °C whereas the head flux load applied on the glazing surface as 261.38 W/m<sup>2</sup> on 6<sup>th</sup> of April. According to the numerical simulation results, the maximum temperature on the glazing surface was obtained 44.75°C for given parameters (Fig. 6). In the experimental study, the maximum temperature measured on the sun exposed surface of the test room was 44.4°C on 6<sup>th</sup> of April (Fig. 3).

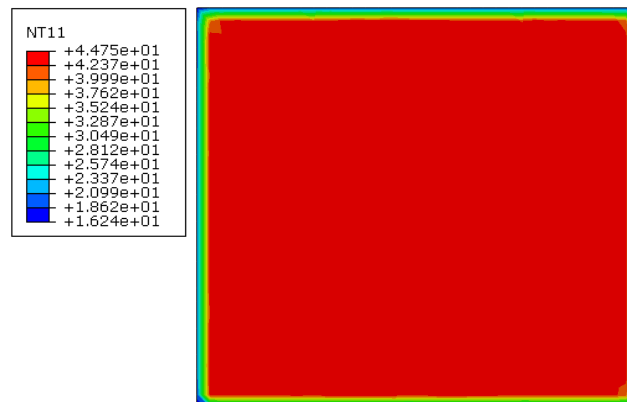


**Figure 6:**  
Temperature distribution on the glazing surface



The thermal wall temperatures were measured on each side for the thermal wall (interior and exterior surfaces) at four points and all these four points were located a meter away from the near wall edges. Therefore, same reference nodes (red dots in Figure 7 represent the reference nodes of thermocouples) and another additional center node were similarly chosen in the numerical analysis to evaluate the temperature values correctly (Fig. 7). The mean values of these 5 nodes were calculated as 42.15°C and 28.97°C for the interior and exterior surfaces, respectively. Side-section view of the thermal wall is also illustrated in order to visualize heat flow through the wall. Experimental measurements for the same surfaces were 44.1°C and 27.6°C on interior and exterior surfaces of the wall.

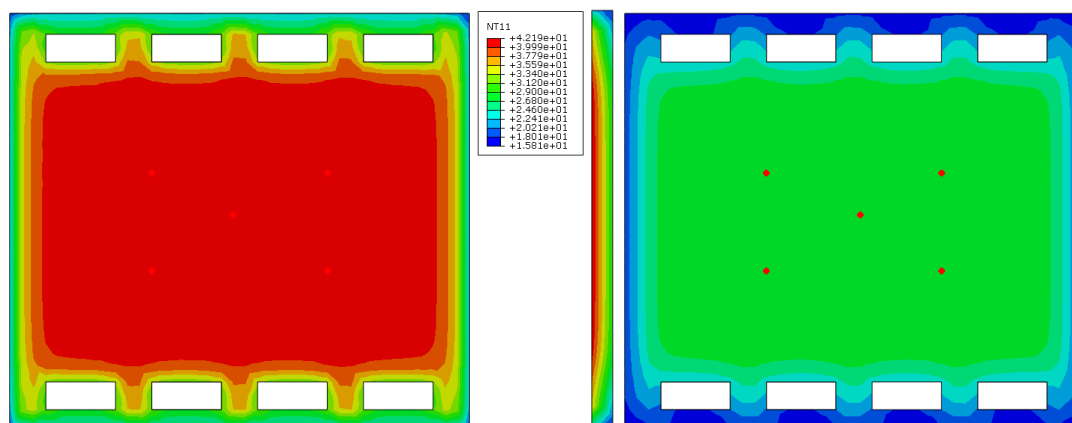


**Figure 7:**  
*Temperature distribution on interior surface (left), inside wall (middle), and exterior surface (right) of TW*

The very same experimental setup was verified in aforementioned research work (Kaya et al., 2021) by employing solar ray tracing algorithm in ANSYS Fluent without defining any additional heat flux load on surfaces. Transient heat transfer simulations were commenced at 13:00 and continued until 19:00 on 6<sup>th</sup> of April when the maximum temperatures were expected. Obtained maximum temperatures on glazing and Trombe wall surfaces were quite similar to FEM and experimental results that is either using FEM with proposed additional heat flux loads or program controlled CFD solar calculator module have presented satisfying results similar to the real measurements.

In the next section, numerically verified model of the Trombe wall system was used in evaluating energy saving potential of residential buildings for three cities with different climate regions in Turkey.

## 5. INVESTIGATION THE CONTRIBUTION OF THE TROMBE WALL TO ENERGY CONSERVATION

The Turkish Standard (TS825, 2013), Thermal Insulation Requirements for Buildings, defines five different degree-day regions in Turkey. The Region I includes the southern cities such as Antalya, Mersin and Adana correspond to hottest cities with temperate climate. As the region number increases, the colder climate it gets associated with continental climate. In this study, three different cities namely Antalya, Istanbul and Ankara were chosen as examples to characterize different day-degree regions that correspond to the Region I, II and III, respectively.

The energy efficiency of the TW is examined for the month of February for these three cities. Therefore, similar to the estimated solar radiation and ambient temperature values obtained for the month of April (Fig. 4), all parameters including ambient temperature and solar radiation values were recalculated for Antalya, Istanbul and Ankara to be used in numerical studies (Fig. 8).

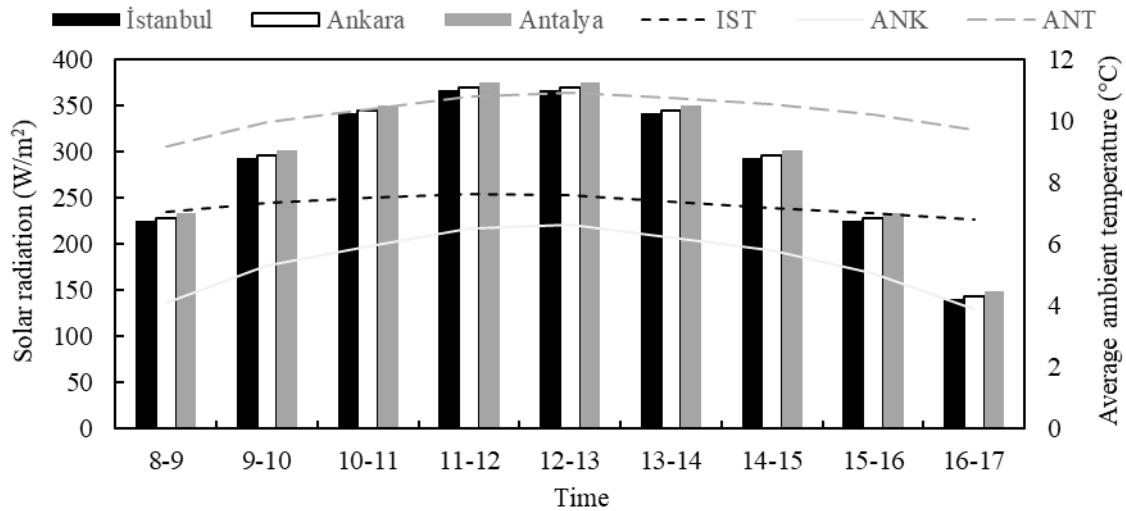


**Figure 8:**

*Solar radiation and ambient temperature values for Region I, II and III cities for the month of February*

According to the ASHRAE-55 (ANSI/ASHRAE, 2017) Standard, thermal comfort zone is defined in the range between 20.0-24.0 °C. In this manner, minimum required indoor temperature to be reached for the purposes of thermal comfort was assumed to be 22.0 °C. In numerical studies, the maximum ambient temperature values were set to be 10.80 °C, 7.63 °C and 6.52 °C for Antalya, Istanbul and Ankara, respectively (Fig. 8) and the maximum exterior surface temperatures of the TW are obtained as 20.73 °C, 19.13 °C and 18.08 °C (Fig. 9, 10 and 11). The minimum required temperature for the city Antalya (Region I) is equal to  $22.0 - 20.73 = 1.27$  °C whereas the difference is  $22.0 - 19.13 = 2.87$  °C for Istanbul and is  $22.0 - 18.08 = 3.92$  °C for Ankara. Considering that the minimum required temperature differences are provided by means of heating, ventilation and air conditioning (HVAC) systems, the percentage of energy saving in Antalya is  $(20.73 - 10.80) / (22.0 - 10.80) \times 100\% = 88.66\%$  while that in Istanbul is  $(19.13 - 7.63) / (22.0 - 7.63) \times 100\% = 80.03\%$  and in Ankara is  $(18.08 - 6.52) / (22.0 - 6.52) \times 100\% = 74.68\%$  (Fig. 9).

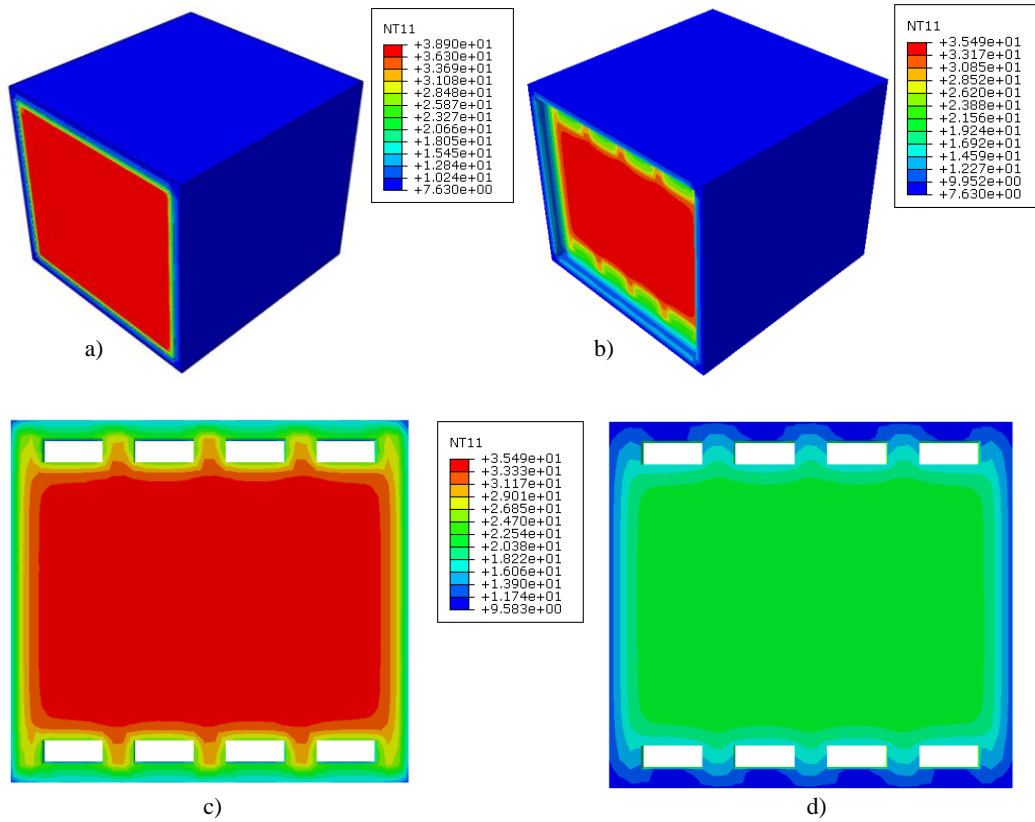


**Figure 9:**  
 Temperature results of the simulation model for Istanbul, a) with and b) without glazing c) interior and d) exterior surfaces of the TW

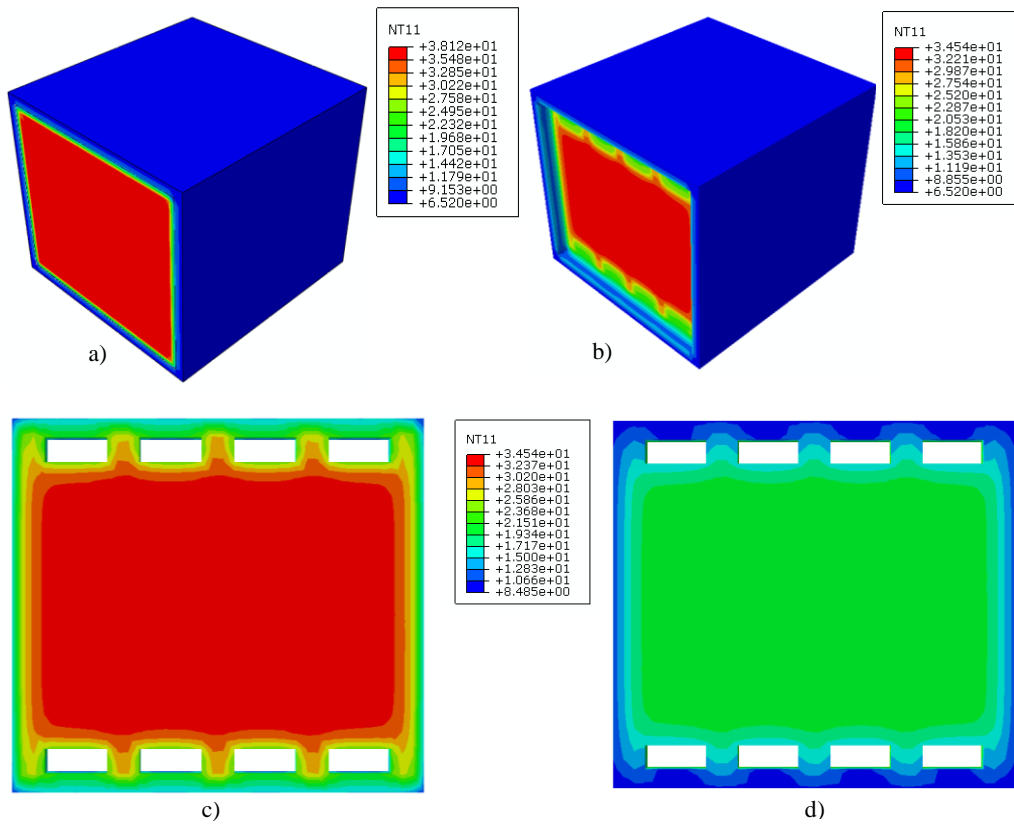


**Figure 10:**  
*Temperature results of the simulation model for Ankara, a) with and b) without glazing c) interior and d) exterior surfaces of the TW*

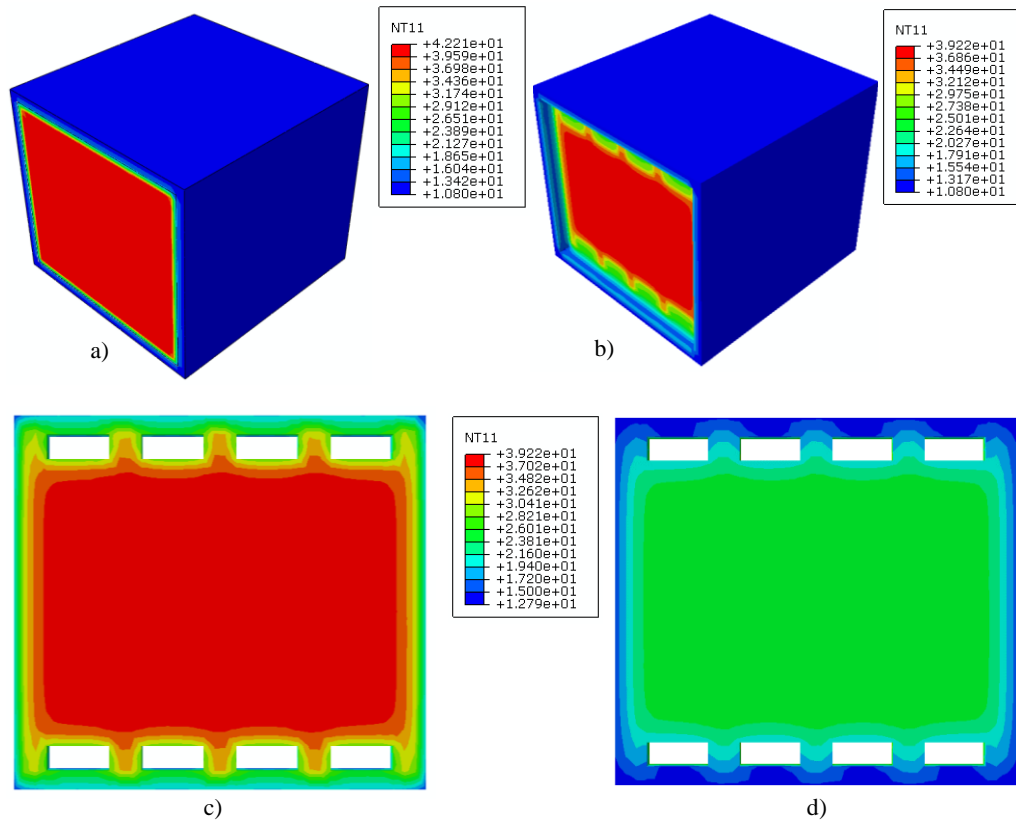


**Figure 11:**  
 Temperature results of the simulation model for Antalya, a) with and b) without glazing c) interior and d) exterior surfaces of the TW

The Energy Market Regulatory Authority of Turkish Republic (EPDK, 2021) reported electricity costs for the month February, 2020 on city basis. Electricity consumption in Antalya was  $3.92 \times 10^8$  kWh while that in Istanbul and Ankara were  $1.01 \times 10^9$  and  $2.71 \times 10^8$  kWh, respectively. If the energy saving calculations are evaluated according to the numerical results obtained by employing indoor temperature as  $22.0 \text{ }^\circ\text{C}$  with respect to ASHRAE-55 and PGIS ambient temperature values, the 88.66% of energy saving for Antalya become approximately equal to  $3.48 \times 10^8$  kWh of energy saving. This value becomes  $8.08 \times 10^8$  kWh of energy saving for Istanbul and  $2.02 \times 10^8$  kWh for Ankara, as well (Fig. 12).

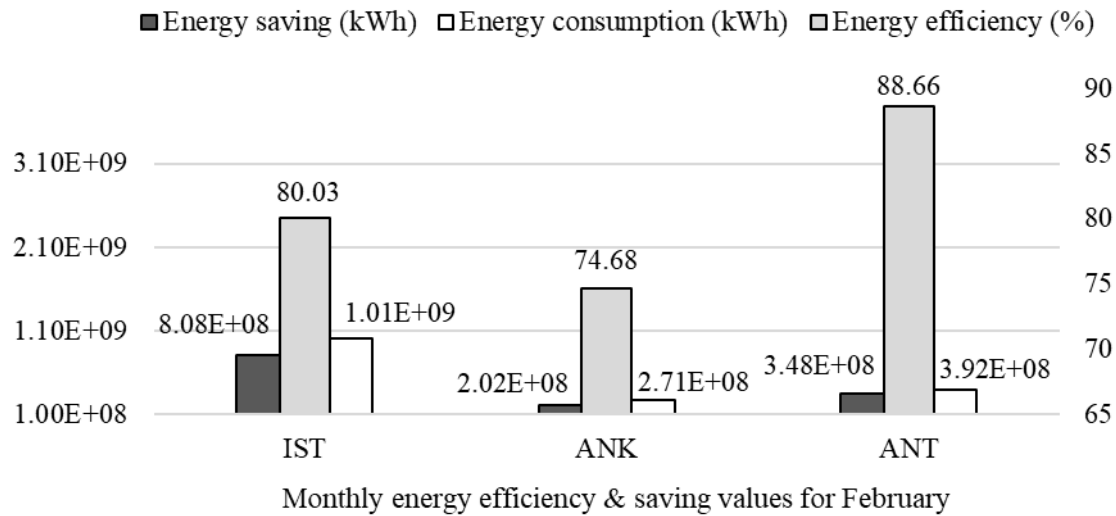


**Figure 12:**  
Energy efficiency and saving values for the month of February 2020

## 6. CONCLUSIONS

Computational fluid dynamics programs are highly efficient and practical tools which are used for designing Trombe wall and solar energy-based systems. Available solar load module and boundary conditions (semi-transparent and opaque) enable the users to simulate glazing and wall materials with accompanying properties such as transmissivity, reflectivity, and absorptivity.

In this research work, a three-dimensional Trombe wall model was developed by using finite element method to obtain realistic results without employing neither solar load module or semi-transparent and opaque boundary conditions but shell and solid elements. For this purpose, a simple approach was proposed by defining estimated solar heat flux loads on glazing surface and additional heat flux on surfaces where solar radiation is incident on.

For the validation studies, a 3D FEM model was modeled identical to a previous experimental test room which was built for investigating thermal performance of a Trombe wall system through temperature measurements. It is seen that the proposed FEM model results are in a good agreement with the observed results. In addition, the very same test room model which was validated due to CFD method by adopting solar ray tracing model in a previous literature work presented similar results with both experimental and FEM models.

Besides, numerically verified model of the Trombe wall system was used in evaluating energy saving potential of residential buildings for Antalya, Istanbul and Ankara cities representing different climate regions in Turkey. A steady state heat transfer analysis was conducted to provide thermal comfort conditions given in ASHRAE standard. As for energy savings, indoor temperature of the model is increased up to 20.73 °C, 19.13 °C and 18.08 °C for Antalya, Istanbul and Ankara, respectively, that is the percentage of the energy saving of these three cities are 88.66, 80.03 and 74.68% to obtain 22.0 °C of required indoor temperature. This also corresponds to 3.48x10<sup>8</sup> kWh of energy saving for Antalya for the month of February 2020 and, 8.08x10<sup>8</sup> and 2.02x10<sup>8</sup> kWh of energy savings for Istanbul and Ankara, respectively.

By this study, it is also proven that the FEM model is able to output results in accordance with the real time measurements of an experimental study and can be used as an alternative solution method to CFD when dealing with problems including solar radiation and transmittivity.

## CONFLICT OF INTEREST

The authors acknowledge that there is no known conflict of interest or common interest with any institution / organization or person.

## AUTHOR CONTRIBUTION

Ercan Şerif Kaya contributed 100% at every stage of the study.

## REFERENCES

1. Gupta, N., and Tiwari, GN. (2016) Review of passive heating/cooling systems of buildings. *Energy Science and Engineering*, (4), 305-333. <https://doi.org/10.1002/ese3.129>
2. Yilmaz, Z., and Kundakci, A.B. (2018) An Approach for energy conscious renovation of residential buildings in Istanbul by Trombe Wall system, *Building and Environment*, (43), 508-517. <https://doi.org/10.3763/asre.2007.5041>
3. Stazi, F., Mastrucci, A., and Perna, C.D. (2012) The behavior of solar walls in residential buildings with different insulation levels: An experimental and numerical study, *Energy and Buildings*, (47), 217-229. <https://doi.org/10.1016/j.enbuild.2011.11.039>
4. Gan, G. (1998) A parametric study of Trombe walls for passive cooling of buildings, *Energy and Buildings*, (27), 37-43. [https://doi.org/10.1016/S0378-7788\(97\)00024-8](https://doi.org/10.1016/S0378-7788(97)00024-8)
5. Ozbalta, T.G., and Kartal, S. (2010) Heat gain through Trombe wall using solar energy in a cold region of Turkey, *Scientific Research and Essays*, (5), 2768-2778.
6. Fang, X., and Li, Y. (2000) Numerical simulation and sensitivity analysis of lattice passive solar heating walls, *Solar Energy*, (69), 55-66. [https://doi.org/10.1016/S0038-092X\(00\)00014-1](https://doi.org/10.1016/S0038-092X(00)00014-1)
7. Briga, A.S., Martins, A., Cunha, J.B., Lanzinha, J.C., and Paiva, A. (2014) Energy performance of Trombe walls: adaptation of ISO 13790:2008(E) to the Portuguese reality, *Energy and Building*, (74), 111-119. <https://doi.org/10.1016/j.enbuild.2014.01.040>
8. Demirbilek, F.N., Yalciner, U.G., Ecevit, A., Sahmali, E., and Inanici, M. (2003) Analysis of the thermal performance of a building design located at 2465 m: Antalya- Saklikent National Observatory guesthouse, *Building and Environment*, (38), 177-184. [https://doi.org/10.1016/S0360-1323\(02\)00015-X](https://doi.org/10.1016/S0360-1323(02)00015-X)
9. Xiong, Q., Alshehri, H. M., Monfaredi, R., Tayebi, T., Majdoub, F., Hajjar, A., ... & Izadi, M. (2021). Application of Phase Change Material in Improving Trombe Wall Efficiency: An up-to-date and Comprehensive Overview. *Energy and Buildings*, 111824. <https://doi.org/10.1016/j.enbuild.2021.111824>
10. Duan, S., Li, H., Zhao, Z., & Wang, L. (2021). Investigation on heating performance of an integrated phase change material Trombe wall based on state space method. *Journal of Energy Storage*, 38, 102460. <https://doi.org/10.1016/j.est.2021.102460>
11. Jaber, S., and Ajib, S. (2011) Optimum design of Trombe wall system in Mediterranean region, *Solar Energy*, (85), 1891-1898. <https://doi.org/10.1016/j.solener.2011.04.025>
12. Kaya, E.S., Aksel, M., Yigitli, S., and Acikara, T.A. (2021) A numerical study on the effect of vent/Wall area ratio on Trombe Wall thermal performance, *Proceedings of the Institution of Civil Engineers - Engineering Sustainability*, 1-14. <https://doi.org/10.1680/jensu.20.00064>

13. ANSYS FLUENT. Theory Guide, ANSYS, Canonsburg PA, 2013.
14. Liu, Y., Wang, D., Ma, C., and Liu, J.A. (2013) A numerical and experimental analysis of the air vent management and heat storage characteristics of a Trombe wall, *Solar Energy*, (91), 1-10. <https://doi.org/10.1016/j.solener.2013.01.016>
15. Hernández, I.L., Xamán, J., Chávez, Y., Hernández, I.P., and Alvarado, R.J. (2016) Thermal energy storage and losses in a room-Trombe wall system located in Mexico, *Energy*, (109), 512-524. <https://doi.org/10.1016/j.energy.2016.04.122>
16. Bajc, T., Todorovic, M.N., and Svorcan, J. (2015) CFD analyses for passive house with Trombe wall and impact to energy demand, *Energy and Buildings*, (98), 39-44. <https://doi.org/10.1016/j.enbuild.2014.11.018>
17. Blotny, J., and Nems, M. (2019) Analysis of the impact of the construction of a Trombe wall on the thermal comfort in a building located in Wroclaw, Poland, *Atmosphere*, (10), 761-773. <https://doi.org/10.3390/atmos10120761>
18. Simões, N., Manaia, M., and Simões, I. (2021). Energy performance of solar and Trombe walls in Mediterranean climates. *Energy*, 234, 121197. <https://doi.org/10.1016/j.energy.2021.121197>
19. Zhou, A., Wong, K.W., and Lau, D. (2014) Thermal Insulating Concrete Wall Panel Design for Sustainable Built Environment, *The Scientific World Journal*, 279592. <https://doi.org/10.1155/2014/279592>
20. Dimassi, N., and Dehmani, L. (2016) Experimental heat flux analysis of a solar wall design in Tunisia, *Journal of Building Engineering*, (8), 70-80. <https://doi.org/10.1016/j.jobbe.2016.10.001>
21. Yaylacı, M., and Avcar, M. (2020). Finite element modeling of contact between an elastic layer and two elastic quarter planes. *Computers and Concrete*, An International Journal, 26(2), 107-114. <https://doi.org/10.12989/cac.2020.26.2.107>
22. Yaylacı M., Adıyaman E., Öner E. and Birinci A., (2020). Examination of analytical and finite element solutions regarding contact of a functionally graded layer, *Structural Engineering and Mechanics*, 76(3), 325-336. <https://doi.org/10.12989/sem.2020.76.3.325>
23. Oğus, G. (2013). Optimization of Trombe Wall Performance Using Computational Fluid Dynamics and Building Energy Simulation, MSc Dissertation, Istanbul Technical University.
24. [https://re.jrc.ec.europa.eu/pvg\\_tools/en/tools.html#MR](https://re.jrc.ec.europa.eu/pvg_tools/en/tools.html#MR) , Erişim Tarihi: 09.01.2021, Konu: PGIS, Photovoltaic Geographical Information system, Average Solar Radiation Tool.
25. Liu, B., and Jordan, R. (1961) Daily insolation on surfaces tilted towards the equator, *ASHRAE Journal* (10), 53-59.
26. DIN 4701. (1980) Rules for calculating heating requirements of buildings (in German), Beuth Berlin.
27. TS825. (2013) Thermal insulation requirements in buildings, Turkish Institute for Standards, Turkey.
28. ANSI/ASHRAE Standard 55-2017. (2017)., Thermal Environmental Conditions for Human Occupancy, Atlanta, USA.
29. <https://www.epdk.gov.tr/Detay/Icerik/3-0-23/elektrikaylik-sektor-raporlar> , Erişim Tarihi: 09.01.2021, Konu: EPDK, Republic of Turkish, Energy Market Regulatory Authority.